

A transmission line analogy for the development of equatorial ionospheric bubbles

Archana Bhattacharyya¹ and William J. Burke

Air Force Research Laboratory, Hanscom Air Force Base, Massachusetts

Abstract. The Pedersen conductivity of the conjugate E regions couples to the equatorial F region through geomagnetic field lines and plays an important role in the development of equatorial spread F bubbles. Earlier work has suggested that the coupling between the E and F regions is effected through field-aligned currents (FACs). However, these currents have not yet been explicitly introduced into theoretical models. This paper considers oppositely propagating Alfvén waves which are launched by equatorial F region perturbations as carriers of FACs and transverse polarization currents. A transmission line analogy is drawn, with the E region loads at the two ends and the generator in the equatorial F region. The currents which flow through the E regions depend on the plasma density of the propagation medium in which the transmission line is immersed. We conclude that whereas small angles between the solar terminator and the magnetic meridian favor the growth of equatorial bubbles, an increase in the plasma density of the propagation medium and a higher altitude of the equatorial F layer allow greater relaxation of the restriction imposed by the E region conductivities on the growth of equatorial bubbles.

1. Introduction

The generation of field-aligned equatorial plasma bubbles is a postsunset phenomenon in which the day-night asymmetry is attributed to the conductivity of the two conjugate E regions which connect through the equatorial F layer [Kelley, 1989]. The development of the equatorial bubbles is caused by the growth of a Rayleigh-Taylor (R-T) instability on the bottomside of the F layer, where vertical plasma density gradients exist. The basic picture was extended by Zalesak *et al.* [1982] to include E region Pedersen conductivity effects. Their numerical simulation of the nonlinear evolution of bubbles used a “three-layer” model in which all the plasma in the vicinity of the equatorial F region was compressed into an equatorial plane, while the remaining plasma was compressed into two conjugate E layers. They showed that E region Pedersen conductivity retarded bubble growth. Observationally, equatorial scintillations and range spread F data indicate that small angles between the sunset terminator and the magnetic meridian favor the development of equatorial bubbles [Tsunoda, 1985; Abdu *et al.*, 1992]. This also points to

the importance of the coupling of the equatorial F region with the conjugate E regions through field-aligned currents (FACs) as considered by Zalesak *et al.* [1982]. A number of recent studies [Basu *et al.*, 1996; Weber *et al.*, 1996] of equatorial spread F (ESF) have indicated that a full three-dimensional picture is required to understand the nonlinear evolution of ESF bubbles. However, because of the complexity of the problem, the magnetic flux tube integrated approach has been used as an approximation in simulations of the nonlinear evolution of equatorial bubbles [Zalesak *et al.*, 1982; Keskinen *et al.*, 1998]. In this approach, FACs do not appear explicitly.

Electromagnetic characteristics of updrafting equatorial bubbles reported by Aggson *et al.* [1992] suggest that FACs are carried by Alfvén waves generated in the equatorial F region. This concept was previously used in a physical description of time-dependent magnetosphere-ionosphere coupling [Kan and Sun, 1985]. Enhanced magnetospheric convection gives rise to pairs of oppositely propagating Alfvén waves. Reflection of the Alfvén waves from the ionosphere is required for equilibrium closure of FACs coupling the generator to the load. The current density carried by an Alfvén wave, as given in equation (2) of Kan and Sun [1985], is divergence-free since the FACs carried by Alfvén waves self-consistently close across magnetic field lines by the polarization currents flowing along the wave front. Keskinen *et al.* [1998] were the first to recognize the importance of ion-polarization currents and included them in

¹Permanently at Indian Institute of Geomagnetism, Mumbai, India.

Copyright 2000 by the American Geophysical Union.

Paper number 1999JA000458.
0148-0227/00/1999JA000458\$09.00

simulations of the nonlinear evolution of equatorial bubbles. This introduced an effective capacitance into their theoretical framework and an effective relaxation time, since polarization currents tend to slow down the decay of electric fields through Pedersen currents. The relaxation time was given by the ratio of an effective capacitance to the Pedersen conductivity of the region, with the effective capacitance itself determined by the dielectric constant of the plasma which depends on the Alfvén speed. However, electrostatic approximation adopted by *Keskinen et al.* [1998] did not consider polarization currents flowing across field-line segments between the equatorial F region and conjugate E regions. Here, Alfvén waves carry field-aligned and polarization currents so that the total current is divergence-free.

In the present study we postulate that the equatorial F region and the conjugate E regions are coupled by FACs carried by Alfvén waves during equatorial bubble development. Partial reflection of these Alfvén waves at the conjugate E regions matches the generator to the loads. A model based on a transmission line analogy is introduced in section 2 to describe Alfvén wave propagation between the generator and load regions. *Sato and Holzer* [1973] introduced similar transmission line circuit considerations for describing electrical coupling between the high-latitude ionosphere and the magnetosphere. In this they integrated over the distributed inductance, capacitance, and resistance of the individual flux tubes to determine their lumped circuit characteristics. The lumped impedances provide benchmarks against which the present model can be compared. Our study differs from *Sato and Holzer* [1973] in that they did not consider Alfvén wave transmission. They also allowed for field-aligned potential drops which are more appropriate in describing the ionosphere at auroral rather than equatorial latitudes.

The present formulation treats ion-polarization currents not only near the equator, but also between the F layer and conjugate E regions where contributions from Pedersen and gravitational currents are less important. In section 3 we identify the generator in the perturbed equatorial F layer along with an equivalent network using the expression for current density derived for that region. Oppositely propagating Alfvén waves are launched from the generator region and are partially reflected at the conjugate E regions. The Alfvén waves carry the FACs that electrically couple the F and E regions. At intermediate altitudes between the F and E regions wave-induced polarization currents close the FACs. The linear stability of the total circuit is investigated in section 4. The development of equatorial bubbles is governed not only by positive growth rates, but also by how the perturbation electric field satisfies the conditions imposed by the current continuity in the conjugate E regions. The E region impacts the growth of F region perturbations through Alfvén wave reflection. The conditions that this imposes on perturbation amplitudes are discussed in section 5. Finally, we examine the effects on bubble development exerted by the

background plasmas in which transmission lines are immersed in the light of growth conditions suggested by ground-based observations (section 6).

2. Model

Consider a Cartesian coordinate system in which the x , y , and z axes point vertically upward, eastward, and northward, respectively. We approximate the geomagnetic field \vec{B}_0 as uniform and northward. The electric field \vec{E} and the magnetic induction \vec{B} satisfy Maxwell's equations:

$$\vec{\nabla} \cdot \vec{E} = e(n_i - n_e)/\epsilon_0 \quad (1)$$

$$\vec{\nabla} \cdot \vec{B} = 0 \quad (2)$$

$$\vec{\nabla} \times \vec{E} = -\frac{\partial \vec{B}}{\partial t} \quad (3)$$

$$\vec{\nabla} \times \vec{B} = \mu_0 \left(\vec{j} + \epsilon_0 \frac{\partial \vec{E}}{\partial t} \right), \quad (4)$$

where n_i and n_e are the densities of ions and electrons, respectively, with $n_i = n_e = n_0$ under equilibrium conditions. The two-fluid equations which describe the behavior of the equatorial F region plasma are the continuity and momentum equations for ions and electrons:

$$\frac{\partial n_j}{\partial t} + \vec{\nabla} \cdot (n_j \vec{v}_j) = -\nu_R n_j \quad (5)$$

$$n_j m_j \left(\frac{\partial \vec{v}_j}{\partial t} + \vec{v}_j \cdot \vec{\nabla} \vec{v}_j \right) = -\kappa_B T_j \vec{\nabla} n_j + n_j m_j \vec{g} + n_j q_j (\vec{E} + \vec{v}_j \times \vec{B}) - n_j m_j \nu_j (\vec{v}_j - \vec{U}) \quad (6)$$

where the subscript j denotes ions (i) or electrons (e); m_j , q_j , T_j , and \vec{v}_j represent the mass, charge, temperature, and velocity, respectively, of each species; ν_R is the recombination rate; ν_j is the collision frequency of each species with neutrals; and \vec{U} is the neutral wind velocity.

In the equatorial F region, for both ions and electrons, the ratio κ_j of gyrofrequency $\Omega_j = q_j B_0 / m_j$ to collision frequency ν_j has a magnitude much greater than 1, while $|\kappa_e| \gg |\kappa_i|$. In deriving the electron velocity from the electron momentum equation, inertial effects and collisions are ignored. For ions, the effects of ion-neutral collisions as well as the inertial term are retained in the ion momentum equation to obtain the ion velocity correct to first order in an iterative calculation [*Keskinen et al.*, 1998]. The ambient electric field \vec{E}_0 is assumed to be uniform and to have only a y component. The eastward current density in the equatorial F region is then obtained as

$$j_y = e[n_i \mu_P^i - n_e \mu_P^e](E_0 + E_{1y}) + \frac{n_i m_i g}{B_0} + \frac{1}{\mu_0 V_A^2} \left(\frac{\partial}{\partial t} + v_{i0y} \frac{\partial}{\partial y} \right) E_{1y}, \quad (7)$$

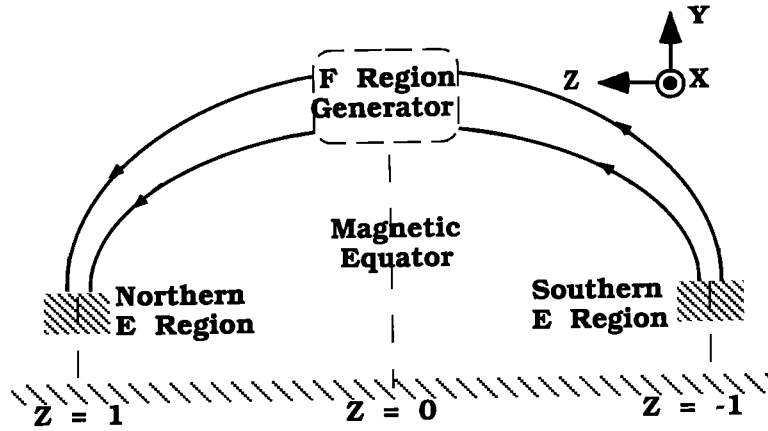


Figure 1. Schematic of the equatorial F region generator coupled to the conjugate E regions in the Northern and Southern Hemispheres through geomagnetic field lines.

where E_{1y} is a perturbation electric field. Here effects of the neutral wind have been incorporated into E_0 ; e is the unsigned electron charge; $\mu_P^j \approx \nu_j/B_0\Omega_j$ is the Pedersen mobility of each species in the F region, where $|\mu_P^i| \gg |\mu_P^e|$; $V_A = \sqrt{(B_0^2/\mu_0 n_0 m_i)}$ is the Alfvén speed in this region; and v_{i0y} is the zeroth-order ion velocity in the eastward direction, given by

$$v_{i0y} = \mu_P^i E_0 + \frac{g}{\Omega_i}. \quad (8)$$

A density perturbation in the bottomside equatorial F layer causes charges to pile up on the edges of the perturbation because the gravitational current in (7) is not divergence-free. As a result, polarization electric fields \vec{E}_1 build up. In the presence of an upward density gradient, an eastward directed \vec{E}_1 causes plasma to drift upward in depleted regions and downward where the plasma density is enhanced. Thus perturbations grow as an R-T instability [Ossakow, 1981]. In earlier models of equatorial bubble development caused by the R-T instability, only electrostatic perturbations were considered. In the present model, time-varying electric field perturbations are associated with magnetic field fluctuations through Maxwell's equations, and a transmission line analogy is drawn to describe the propagation of the electromagnetic perturbations from the equatorial F region to conjugate E regions along geomagnetic field lines.

In our transmission line analogy, magnetic flux tubes are aligned along the z direction to form parallel, perfect conductors, as depicted in Figure 1. Flux tube cross sections are arbitrarily shaped and are assumed to be independent of z , so that the parallel component of the electric field E_z vanishes everywhere. This is a fundamental difference between the present formalism and that of Sato and Holzer [1973], who assumed that $E_z \neq 0$. We also assume that properties of the background ionospheric plasma in the regions between the generator in the equatorial F region and the E region loads at the two ends do not change with z . Under these conditions, solutions of Maxwell's equations are partially separable.

Thus, if a perturbation in the generator region launches oppositely propagating Alfvén waves with electric field perturbations $\vec{E}_{1\pm}$ and the corresponding magnetic field perturbations $\vec{H}_{1\pm} = \vec{B}_{1\pm}/\mu_0$, where the plus and minus signs represent Alfvén waves propagating parallel and antiparallel, respectively, to \vec{B}_0 , these may be written as products of functions of the transverse coordinate $\vec{\rho}$, the longitudinal coordinate z , and time t . The electric field of an Alfvén wave is related to its magnetic field through $\vec{E}_{1\pm} = -\vec{v} \times \vec{B}_0$, where $\vec{v} = \mp \vec{B}_{1\pm} V_{Am}/B_0$ is the fluid velocity and $V_{Am} = B_0/(\mu_0 n_m m_i)^{1/2}$ is the Alfvén speed in the background plasma of unperturbed density n_m , which may be different from the equilibrium density n_0 in the generator region. It is assumed that the perturbation electric field is along the y axis and is independent of x , such that it has the form

$$\vec{E}_{1\pm} = F(y)V_{\pm}(z,t)\hat{y}. \quad (9)$$

The magnetic field perturbation associated with Alfvén waves traveling up and down the geomagnetic field lines is perpendicular to both \vec{B}_0 and $\vec{E}_{1\pm}$ and may be written as

$$\vec{H}_{1\pm} = G(y)I_{\pm}(z,t)\hat{x}. \quad (10)$$

Assuming the perturbation in the generator region to have an east-west wavelength $2\pi/k_y$, the functions $F(y)$ and $G(y)$ have the form

$$F(y) = G(y) = e^{ik_y y}. \quad (11)$$

The relationship between the electric and magnetic fields of an Alfvén wave implies that

$$V_{\pm} = \mp \mu_0 V_{Am} I_{\pm}. \quad (12)$$

The current density of the Alfvén wave, $\vec{j}_A = \vec{\nabla} \times \vec{H}_{1\pm}$, may be expressed in terms of the electric field as follows [Kan and Sun, 1985]:

$$\vec{j}_A = \mp \Sigma_A [-\hat{B}_0(\vec{\nabla} \cdot \vec{E}_{1\pm}) + (\hat{B}_0 \cdot \vec{\nabla})\vec{E}_{1\pm}], \quad (13)$$

where \hat{B}_0 is a unit vector along the geomagnetic field

and $\Sigma_A = (\mu_0 V_{Am})^{-1}$. The first term in (13) is the field-aligned current carried by the Alfvén wave, while the second term represents a polarization current which flows across field lines along the propagating wave front. The field-aligned current is now determined by $\vec{\nabla} \cdot \vec{E}_{1\pm}$, which characterizes the perturbation, and by Σ_A , which characterizes the propagation medium. In this approach, therefore, it is not necessary to determine explicitly the impedance associated with the circuit in order to deduce the field-aligned current, as was required in the formalism of *Sato and Holzer* [1973]. Since $\vec{\nabla} \cdot \vec{j}_A = 0$ in the propagation medium, the field-aligned current of an Alfvén wave closes across field lines through the polarization current along the wave front. In the E region FACs close through Pedersen currents and partially reflected Alfvén waves [*Kan and Sun*, 1985].

3. Characterization of the Equatorial F Region Generator

The gravitational current which appears in (7) may be identified with a current source in the equatorial F region. A resistive element, represented by the Pedersen resistivity of the equatorial F region, and a capacitance associated with the polarization current in that region are connected in parallel with this current source. The generator in the equatorial F region is now represented by an equivalent network consisting of these three elements connected in parallel such that the current which arises from the generator is the sum of the currents flowing through each of these elements. Poynting's theorem is invoked later to justify use of the term "generator" for the bottomside equatorial F region in the initial phase of bubble development. Outside the generator region the gravitational drift and, hence, the gravitational current are neglected.

The other regions of substantial Pedersen current are lumped into the conjugate E regions which are assumed to extend from $z = l$ to $z = l + \Delta z$ in the Northern Hemisphere and from $z = -l - \Delta z$ to $z = -l$ in the Southern Hemisphere. These are considered to be passive loads. In this respect the present model is similar to the three-layer models used by *Zalesak et al.* [1982] and *Keskinen et al.* [1998]. However, we do not consider all the plasma to be compressed into three layers, and we allow plasma of uniform, zeroth-order density n_m to be present in the regions between the generator and loads, such that a field-aligned current j_z may be carried by Alfvén waves propagating in this plasma

$$j_z = (\vec{\nabla} \times \vec{H}_1)_z = -\frac{\partial H_{1x}}{\partial y} \quad (14)$$

along with a polarization current which flows across the geomagnetic field lines, as described in (13). It will be seen below that the polarization current carried by the Alfvén wave may be identified with the current j_{y0} ob-

tained from (7) when the gravity and Pedersen mobility terms are ignored

$$j_{y0} = \frac{1}{\mu_0 V_{Am}^2} \frac{\partial E_{1y}}{\partial t} = \epsilon_0 \frac{c^2}{V_{Am}^2} F \frac{\partial V}{\partial t}, \quad (15)$$

where $c = (\mu_0 \epsilon_0)^{-1/2}$ is the velocity of light in free space. With \vec{E}_1 and \vec{H}_1 given by (9) and (10), respectively, where the plus or minus sign is ignored for the present, (3) and (4) yield

$$F \frac{\partial V}{\partial z} = \mu_0 G \frac{\partial I}{\partial t} \quad (16)$$

$$G \frac{\partial I}{\partial z} = j_y + \epsilon_0 F \frac{\partial V}{\partial t}. \quad (17)$$

In the propagation medium $j_y = j_{y0}$, and with a typical Alfvén speed, V_{Am} of a few hundred kilometers per second, it is seen from (15) that the contribution of j_{y0} is much greater than that of the last term on the right side of (17). In the background plasma, (16) and (17) now yield

$$\frac{\partial^2 V}{\partial z^2} = \mu_0 \epsilon_m \frac{\partial^2 V}{\partial t^2} \quad (18)$$

$$\frac{\partial^2 I}{\partial z^2} = \mu_0 \epsilon_m \frac{\partial^2 I}{\partial t^2}, \quad (19)$$

where $\epsilon_m = \epsilon_0 \epsilon_r$. The dielectric constant of the background plasma ϵ_r is given by

$$\epsilon_r = 1 + \frac{c^2}{V_{Am}^2}. \quad (20)$$

The solutions of (18) and (19), which represent Alfvén waves propagating parallel or antiparallel to \vec{B}_0 , are of the form $e^{i(\pm k_z z - \omega t)}$, where k_z is related to ω by

$$k_z^2 = \mu_0 \epsilon_m \omega^2. \quad (21)$$

As $c \gg V_{Am}$, a perturbation would propagate along the z axis with the Alfvén speed. With V and I related through (12), it is seen that j_{y0} given by (15) is the polarization current carried by the Alfvén wave according to (13). Thus the geomagnetic field lines act as transmission lines immersed in the background ionospheric plasma along which the Alfvén waves propagate. Now if we introduce L and C as the inductance and capacitance per unit length of the transmission line, respectively, it is a textbook problem in classical electrodynamics to demonstrate that the product of L and C is given by [*Jackson*, 1975]

$$LC = \mu_0 \epsilon_m. \quad (22)$$

The electric circuit which represents the coupling of the equatorial F region generator network to the conjugate E region loads, through geomagnetic field lines that act as transmission lines, is depicted schematically in Figure 2. R_{EN} and R_{ES} are the resistances associated with the Northern and Southern Hemisphere E regions,

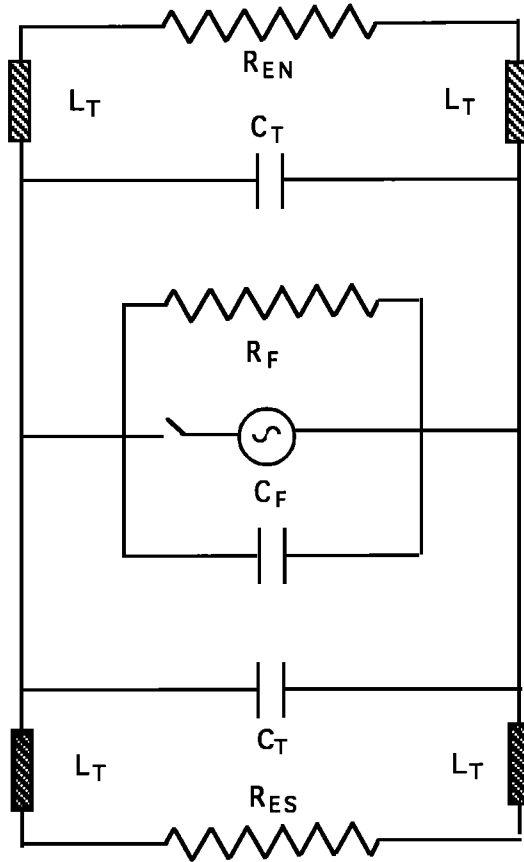


Figure 2. Electric circuit used to represent the coupling of the equatorial F region generator network to the conjugate E regions of resistances R_{EN} and R_{ES} through geomagnetic field lines acting as transmission lines with inductance L_T and capacitance C_T .

respectively, and $L_T = Ll$ and $C_T = Cl$ are the inductance and capacitance, respectively, associated with length l of the geomagnetic field lines which connect the equatorial F region with either of the E regions. As we discussed earlier, in our formalism it is not necessary to obtain the circuit elements in Figure 2 in terms of physical parameters of the ionosphere by introducing assumptions which are not supported by the basic equations (1)-(6), on which the formalism is based. Instead, it is seen that the inductance L and capacitance C per unit length of the transmission line appear in the equations only in the combination LC , which, according to (22), is determined by the electric permittivity ϵ_m of the background ionospheric plasma where the transmission line is immersed. In order to obtain the expression, given in their equation (A4), for the inductance associated with l , *Sato and Holzer* [1973] had to assume a nonvanishing component of the electric field parallel to the geomagnetic field lines. The capacitance associated with l is given by their equation (A14). Thus, according to these two expressions derived by *Sato and Holzer* [1973], the product of the inductance and capacitance per unit length of the geomagnetic field line is given by $LC = 0.18/V_A^2$, where V_A is the Alfvén speed in

the magnetosphere. The factor 0.18 is a result of the approximations introduced by *Sato and Holzer* [1973].

In the background plasma in which the transmission lines are immersed, (18) and (19) have general solutions of the form

$$V(z, t) = [V_+ e^{ik_z z} + V_- e^{-ik_z z}] e^{-i\omega t} \quad (23)$$

$$I(z, t) = [I_+ e^{ik_z z} + I_- e^{-ik_z z}] e^{-i\omega t}, \quad (24)$$

which represent a combination of Alfvén waves propagating parallel and antiparallel to \vec{B}_0 . The generator region is considered to extend from $z = -\Delta z_F$ to $z = +\Delta z_F$ along the geomagnetic field line, where Δz_F is small compared with the wavelength of the perturbation along the field line. Reflections of the Alfvén waves from the E region loads, as well as the generator in the equatorial F region, are considered to be equivalent to closure of the FACs carried into these regions [*Kan and Sun*, 1985]. For current from the source region to remain constant, the field-aligned currents of the incident and reflected Alfvén waves must cancel each other in that region. Thus the field-aligned current which flows at $z = +\Delta z_F$ reduces to zero at $z = 0$ when the Alfvén waves are reflected from the source region. Similarly, the field-aligned current which flows at $z = -\Delta z_F$ also reduces to zero at $z = 0$. Closure of the field-aligned currents requires that in the generator region

$$\frac{\partial j_y}{\partial y} + \epsilon_0 \frac{\partial F}{\partial y} \frac{\partial V}{\partial t} \approx -\frac{j_z(\Delta z_F)}{\Delta z_F} \quad (25)$$

$$\frac{\partial j_y}{\partial y} + \epsilon_0 \frac{\partial F}{\partial y} \frac{\partial V}{\partial t} \approx \frac{j_z(-\Delta z_F)}{\Delta z_F}. \quad (26)$$

These yield

$$\frac{\partial j_y}{\partial y} + \epsilon_0 \frac{\partial F}{\partial y} \frac{\partial V}{\partial t} \approx -\frac{[j_z(\Delta z_F) - j_z(-\Delta z_F)]}{2\Delta z_F}. \quad (27)$$

According to (14), j_z is given by

$$j_z = -ik_y G [I_+ e^{ik_z z} + I_- e^{-ik_z z}] e^{-i\omega t}. \quad (28)$$

Therefore, to first order in $k_z \Delta z_F$,

$$\frac{\partial j_y}{\partial y} + \epsilon_0 \frac{\partial F}{\partial y} \frac{\partial V}{\partial t} = -\left. \frac{\partial j_z}{\partial z} \right|_{z=0}. \quad (29)$$

Hence the generator may be considered to exist at $z = 0$ and (29) represents the current continuity equation which would be obtained from (4). This replaces the current continuity equation $\partial j_y / \partial y = 0$ used in the usual R-T stability analysis [*Kelley*, 1989].

According to Poynting's theorem, the rate at which the mechanical energy of the plasma's $\vec{E}_1 \times \vec{B}_0$ motion is transformed into electromagnetic energy as Alfvén waves is determined by

$$\frac{1}{2} \text{Re}(\vec{j}_A^* \cdot \vec{E}_1) = \frac{1}{2} \text{Re}[(\vec{\nabla} \times \vec{H}_1)^* \cdot \vec{E}_1]. \quad (30)$$

As noted earlier, the current from the source region stays constant provided the field-aligned currents of the incident and reflected Alfvén waves cancel each other, which requires that

$$I_+ + I_- = 0. \quad (31)$$

Use of (12), (13), and (31) in (30) yields at the boundaries of the equatorial F region

$$\frac{1}{2} \text{Re}(\vec{j}_A^* \cdot \vec{E}_1) = -\gamma \epsilon_m [|V_+|^2 + |V_-|^2], \quad (32)$$

where γ is the growth rate of the perturbation in the equatorial F region. Hence this region may be identified with a generator of Alfvén waves when a bubble starts to grow.

4. Stability Analysis

We next consider the linear stability of the system in the presence of small density perturbations in the bottomside equatorial F layer. For consistency, the perturbed electron and ion densities are considered to be different. However, departures from quasi-neutrality are negligible. With perturbations \tilde{n}_i and \tilde{n}_e in ion and electron densities in the equatorial F region generator, and a perturbation E_{1y} in the electric field, and retaining only the terms linear in the perturbations, the ion continuity equation (5) yields

$$\frac{\partial \tilde{n}_i}{\partial t} + \frac{E_{1y}}{B_0} \frac{\partial n_0}{\partial x} + v_{i0y} \frac{\partial \tilde{n}_i}{\partial y} + n_0 \mu_P^i \frac{\partial E_{1y}}{\partial y} = -\nu_R \tilde{n}_i. \quad (33)$$

Since the perturbations are assumed to have an east-west wavelength $2\pi/k_y$, \tilde{n}_i and \tilde{n}_e may be written as

$$\tilde{n}_i = \tilde{n}_{i0} e^{-i\omega t} e^{ik_y y} \quad (34)$$

$$\tilde{n}_e = \tilde{n}_{e0} e^{-i\omega t} e^{ik_y y}. \quad (35)$$

Equation (1) implies that at $z = 0$,

$$ik_y [V_+ + V_-] = \frac{e}{\epsilon_0} [\tilde{n}_{i0} - \tilde{n}_{e0}]. \quad (36)$$

At $z = 0$ the electric permittivity ϵ depends on V_A the Alfvén speed there: $\epsilon = \epsilon_0(1 + c^2/V_A^2)$; and the current continuity equation yields

$$\begin{aligned} & \left[n_0 e M_P - i\epsilon\omega + \frac{ik_y}{\mu_0 V_A^2} \left(\mu_P^i E_0 + \frac{g}{\Omega_i} \right) + \right. \\ & \left. \frac{ik_z^2}{\mu_0 \omega} + ik_y \epsilon_0 \mu_P^e E_0 \right] (V_+ + V_-) = \\ & - \left[e M_P E_0 + \frac{m_i g}{B_0} \right] \tilde{n}_{i0}, \end{aligned} \quad (37)$$

where $M_P = \mu_P^i - \mu_P^e$. The last term in the brackets on the left side of (37) represents the effect of charge

separation, which is negligible compared with the first term. Hence assumption of quasi-neutrality is valid, and this term may be ignored. At $z = 0$ the ion continuity equation (33) yields

$$\begin{aligned} & \left[\frac{1}{B_0} \frac{\partial n_0}{\partial x} + ik_y n_0 \mu_P^i \right] (V_+ + V_-) = \\ & \left[i\omega - \nu_R - ik_y \left(\mu_P^i E_0 + \frac{g}{\Omega_i} \right) \right] \tilde{n}_{i0}. \end{aligned} \quad (38)$$

With the substitution of the right-hand side of (21) for k_z^2 , (37) and (38) yield the dispersion relation

$$A_1 \omega^2 + A_2 \omega + A_3 = 0, \quad (39)$$

where

$$A_1 = \epsilon - \epsilon_m \quad (40)$$

$$A_2 = i \left[\sigma_P^F + i \frac{1}{\mu_0 V_A^2} \frac{k_y g'}{\Omega_i} + A_1 \left(\nu_R + i \frac{k_y g'}{\Omega_i} \right) \right] \quad (41)$$

$$\begin{aligned} A_3 &= \frac{m_i g'}{B_0} \left[\frac{1}{B_0} \frac{\partial n_0}{\partial x} + ik_y n_0 \mu_P^i \right] \\ &- \left(\sigma_P^F + i \frac{1}{\mu_0 V_A^2} \frac{k_y g'}{\Omega_i} \right) \left(\nu_R + i \frac{k_y g'}{\Omega_i} \right). \end{aligned} \quad (42)$$

Here $g' = g + \nu_i E_0/B_0$ includes the effect of an east-west ambient electric field, and $\sigma_P^F = n_0 e M_P$ is the Pedersen conductivity of the equatorial F region. For parameters pertaining to bubble development, $k_y g'/\mu_0 V_A^2 \Omega_i \sim 2 \times 10^{-10}$ mho/m, which is much smaller than σ_P^F , since $\sigma_P^F > 10^{-8}$ mho/m for altitudes below 800 km. Hence that term may be neglected. The capacitance is a measure of the polarizability of the medium, and as noted by *Sato and Holzer* [1973] and *Keskinen et al.* [1998], its form in the present situation would be defined by the polarizability of the plasma in the presence of a magnetic field. A part of the polarization current flowing in the equatorial F region is used in closing the field-aligned current flowing out of that region. Hence, in our formalism, this is associated with the capacitance of the transmission line. The remainder of the polarization current in the equatorial F region is associated with an effective capacitance of the equatorial F region generator. Thus the capacitance C_F of the generator is determined by $(\epsilon - \epsilon_m)$, the effective permittivity of the generator region. For $\epsilon = \epsilon_m$ all of the polarization current that flows in the equatorial F region is required for the closure of the FACs flowing into the background plasma, and the remaining current in the equatorial F region, given by the first two terms on

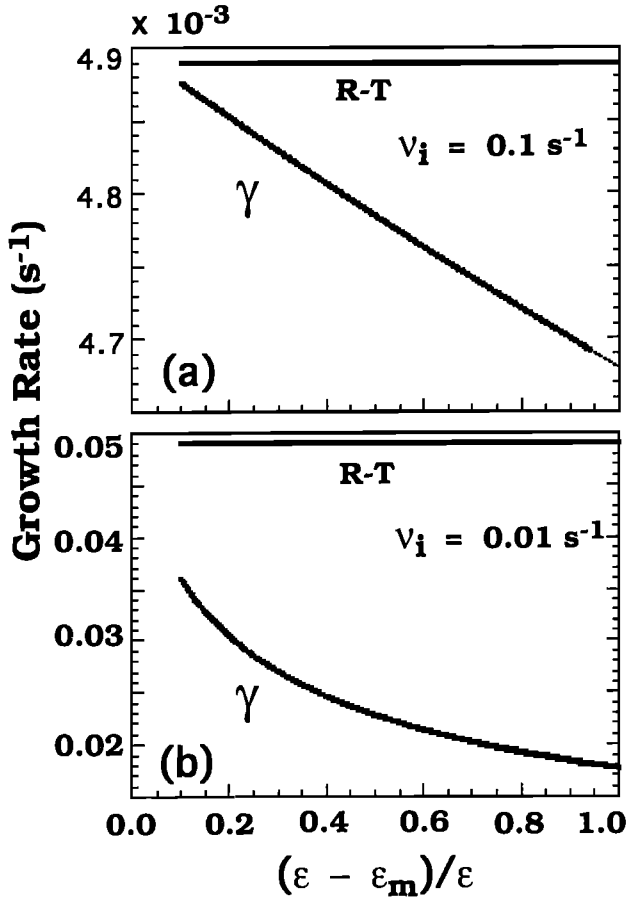


Figure 3. Growth rate of the Rayleigh-Taylor (R-T) instability in the transmission-line mode (solid line) as a function of $(\epsilon - \epsilon_m)/\epsilon$, which is proportional to the capacitance C_F associated with the equatorial F region generator, compared to the growth rate of the usual R-T instability (dashed line), for ion-neutral collision frequencies: $\nu_i = 0.1 \text{ s}^{-1}$ (top) and $\nu_i = 0.01 \text{ s}^{-1}$ (bottom).

the right side of (7), is divergence-free. The capacitance of the generator is zero, and only its resistance governed by the Pedersen conductivity of the equatorial F region comes into the picture. In this situation, (39) reduces to a linear equation in ω and the usual R-T instability is obtained.

For $\epsilon \neq \epsilon_m$, (39) yields two solutions for ω as a function of k_y :

$$\omega = \frac{-A_2 \pm \sqrt{A_2^2 - 4A_1A_3}}{2A_1}. \quad (43)$$

With $V_A = 300 \text{ km/s}$ and $\Omega_i = 200 \text{ Hz}$, the equatorial F region plasma density has a value $n_0 \approx 4 \times 10^{11} \text{ m}^{-3}$. The density gradient scale length in the bottom-side of the equatorial F region is taken to be $L_n = n_0/(\partial n_0/\partial x) = 20 \text{ km}$. The recombination rate $\nu_R = 10^{-5} \text{ s}^{-1}$. For a fixed ϵ , ϵ_m is varied from 0 to 0.9ϵ . It is found that for the range of parameters used, only the solution in (43) with the negative sign yields positive values for γ , the imaginary part of ω ; so this solution

grows with time while the other is damped. In Figure 3 the growth rate γ is plotted as a function of $(\epsilon - \epsilon_m)/\epsilon$ which, as explained above, represents the effective capacitance associated with the equatorial F region generator. Growth rates obtained for the transmission line model are compared with the growth rate for the usual R-T instability ($\epsilon = \epsilon_m$) for two different values of the ion-neutral collision frequency ν_i : 0.1 s^{-1} and 0.01 s^{-1} . The east-west wavelength of the perturbation is considered to be 10 km . The growth rate, which is found to be nearly independent of k_y as in the case of the usual R-T instability, differs noticeably from the R-T growth rate only for $\nu_i < 0.1 \text{ s}^{-1}$. It is to be noted that in our formalism the E region conductivity does not appear in the expression for the growth rate. However, the development of the perturbation depends not only on the growth rate, but also on how the perturbation electric field satisfies the condition imposed by the requirement of current continuity in the conjugate E regions, taking into account the FACs that are carried into the E regions by Alfvén waves. The amplitude of the density perturbation at $z = 0$, \tilde{n}_{i0} , is proportional to $(V_+ + V_-)$, which depends on the relationship between the amplitudes of the waves that propagate parallel and antiparallel to \vec{B}_0 as determined by the “load reflection factor”. The argument is similar to the one used by *Basu and Coppi* [1999] who concluded that the onset of ESF is governed both by the conditions for localization and by a positive growth rate. In the present model, besides a positive growth rate, the criteria for bubble development are the conditions imposed by the conjugate E regions where Alfvén waves are reflected.

5. E Region Boundary Conditions

We assume that Δz along the geomagnetic field in the E regions of both hemispheres is small in comparison with the length of the field lines linking them to the equatorial F region. The field-aligned current which enters the Northern Hemisphere E region at $z = l$ flows there as an eastward Pedersen current j_y^E :

$$j_y^E = \sigma_{PN}^E [E_0 + E_{1y}(z = l)], \quad (44)$$

where σ_{PN}^E is the Pedersen conductivity in the Northern Hemisphere E region. Hence j_z reduces from $j_z(z = l)$ to 0 over a short distance Δz , and current continuity at $z = l$ requires that

$$\frac{\partial j_y^E}{\partial y} - \frac{j_z(z = l)}{\Delta z} = 0. \quad (45)$$

Here any polarization current caused by accumulated charges in the E region is neglected, since Δz is small compared with l . With $j_z(z = l) = -ik_y G(y)I(l, t)$ according to (14), and uniform E region conductivity, (45) yields

$$\Sigma_{PN}^E [V_+ e^{ik_z l} + V_- e^{-ik_z l}] = - [I_+ e^{ik_z l} + I_- e^{-ik_z l}], \quad (46)$$

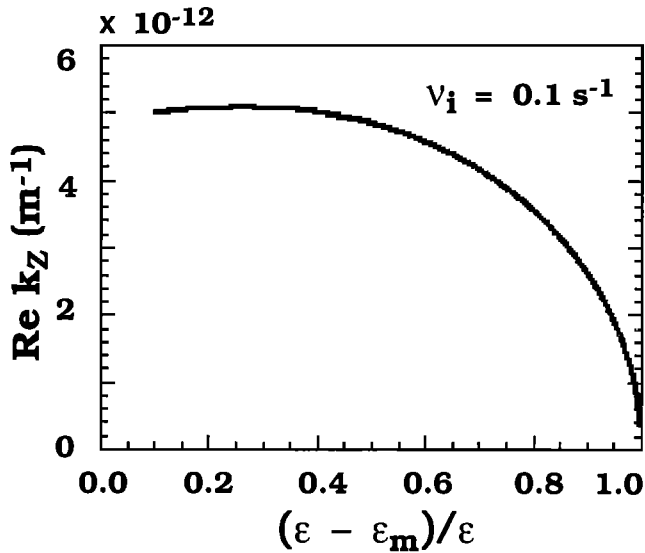


Figure 4. Real part of the wavenumber k_z in the propagation medium as a function of $(\epsilon - \epsilon_m)/\epsilon$.

where $\Sigma_{PN}^E = \sigma_{PN}^E \Delta z$ is simply the flux tube integrated E region Pedersen conductivity in the Northern Hemisphere. Similar arguments hold in the case of the Southern Hemisphere E region located at $z = -l$. However, it must be kept in mind that now the field-aligned current increases from 0 at $z = -l - \Delta z$ to $j_z(z = -l)$ as z increases by Δz . Hence

$$\Sigma_{PS}^E [V_+ e^{-ik_z l} + V_- e^{ik_z l}] = [I_+ e^{-ik_z l} + I_- e^{ik_z l}]. \quad (47)$$

For the current from the source region to stay constant, (31) must be satisfied, which implies that the right sides of (46) and (47) are equal. For the growing mode, k_z determined by (21) has a real part $\leq 10^{-11} \text{ m}^{-1}$ and an imaginary part $< 2 \times 10^{-8} \text{ m}^{-1}$ when $\nu_{in} = 0.1 \text{ s}^{-1}$, as shown in Figures 4 and 5, respectively. Assuming $l \approx 2 \times 10^6 \text{ m}$, it is seen that $(V_+ + V_-) \approx 0$, and hence from (37) or (38), $\tilde{n}_{i0} \approx 0$ unless $\Sigma_{PN}^E \approx \Sigma_{PS}^E \approx 0$, which, then, is a necessary condition for the existence of a density perturbation at $z = 0$. Within the E regions, (12) may not be used to relate V_{\pm} with I_{\pm} , since Alfvén waves do not propagate in those regions.

6. Conclusion

As seen in Figure 3, the growth rate of a perturbation in the equatorial F region tends to decrease as the density of the background ionospheric plasma, in which the transmission line is immersed, decreases from n_0 to 0. The perturbation electric field is larger when the Pedersen resistance R_F of the equatorial F region is higher since Pedersen currents tend to reduce the electric field set up by accumulated charges [Keskinen *et al.*, 1998]. However, if there is a capacitance C_F in parallel with this resistance, a time constant $R_F C_F$ would determine the time taken by the bubble to charge after the generator is switched on. Hence for a given R_F ,

as the capacitance C_F associated with the equatorial F region, which is proportional to $(\epsilon - \epsilon_m)$ increases, the growth rate for the equatorial bubble decreases. As ν_i decreases, the capacitance C_F plays a more important role because of the increased resistance R_F of the equatorial F region. Keskinen *et al.* [1998] came to a similar conclusion regarding the role of polarization currents since the effective relaxation time for changes in the electric field introduced in their formalism was determined by the product $R_F C_F$.

The growth rate alone does not govern the development of equatorial bubbles, as discussed at the end of section 4. The restrictions imposed by the E region loads and the role of the propagation medium in satisfying the required conditions also must be taken into consideration for the development of equatorial bubbles. This may be physically understood as follows. The upward $\vec{j} \times \vec{B}_0$ force on the background plasma arising from the polarization current $\epsilon_m \partial E_{1y} / \partial t$ would be 90° out of phase with the upward velocity of the plasma given by E_{1y} / B_0 provided ω is real. In this situation the oscillations are sustained as the Alfvén waves propagate. However, for a complex ω , this is no longer true. Hence Alfvén waves decay as they propagate from the source to the E regions and back. In the transmission line picture, k_z is determined by the characteristics of the generator and the propagation medium. For a growing mode, the nonzero imaginary part of k_z leads to the decay of Alfvén waves as they propagate from the source to the E regions and back. For a given growth rate, the imaginary part of k_z and hence the rate of Alfvén wave decay with distance increases with increasing ϵ_m . The loss in the signal during propagation along magnetic field lines controls the amount of current. A decrease in the current which flows into the E region helps the growth of equatorial bubbles by preventing the discharge of polarization charges on the bubble walls. Thus there is

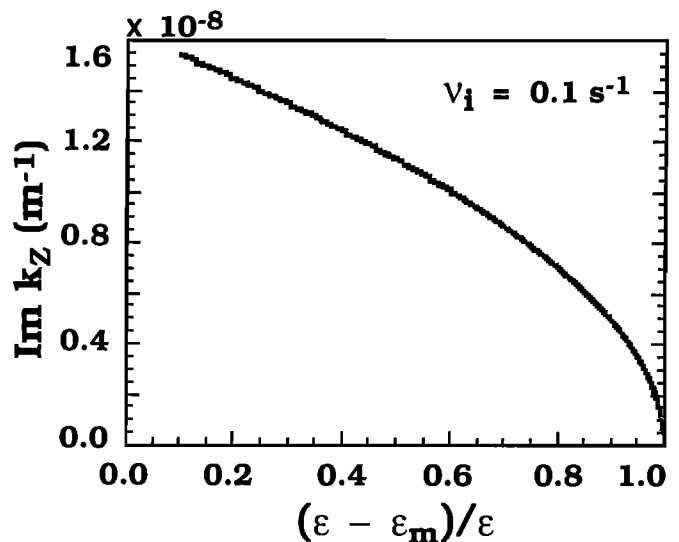


Figure 5. Imaginary part of the wavenumber k_z in the propagation medium as a function of $(\epsilon - \epsilon_m)/\epsilon$.

greater relaxation of the condition $\Sigma_{PN}^E \approx \Sigma_{PS}^E \approx 0$ required for a density perturbation to exist in the equatorial F region as the background plasma density in the region between the generator and the loads increases. From the analogy described in Figure 2, we see that the circuit involves the inductance and capacitance of the transmission line as well as the resistance of the E region. According to (21) and (22),

$$k_z l = (L_T C_T)^{1/2} \omega. \quad (48)$$

Figure 2 indicates that the currents flowing through the E region loads are no longer determined only by the resistances R_{EN} and R_{ES} of the conjugate E regions, but also by the timescale associated with the perturbation in the equatorial F region and the characteristics of the background ionosphere between the equatorial F region and the E regions. The smaller the value of the imaginary part of $(k_z l)$ is, the larger are the currents that flow into and out of the E region loads, for a given resistance of the loads. Thus, in order for the equatorial bubble to develop, the conductivities of the E regions and also the differences between the conductivities have to be smaller, in proportion to the value of $\text{Im}(k_z l)$.

The observed seasonal and longitudinal occurrence patterns of equatorial scintillations are explained on the basis of near-alignment of the solar terminator with the geomagnetic flux tubes as a favorable condition for the growth of ESF bubbles [Tsunoda, 1985]. However, range spread F (RSF) data studied by Abdu *et al.* [1992] indicate that nearly perfect alignment of the terminator with the magnetic meridian tends to be less favorable for bubble growth. Results obtained in the present paper imply that a small angle between the solar terminator and magnetic meridian is an important factor for growth of equatorial bubbles such that it is possible to have $\Sigma_{PN}^E \approx \Sigma_{PS}^E \approx 0$. However, higher ionospheric densities between the equatorial F region and the conjugate E regions may help bubble growth by relaxing this condition. The importance of a large F region vertical plasma drift velocity in the generation and evolution of ESF bubbles has been suggested by Fejer *et al.* [1999] on the basis of long-term radar observations from the Jicamarca observatory. In a number of studies the height of the nighttime F layer has been singled out as the most important parameter in the generation of ESF [Kelley and Maruyama, 1992; Jayachandran *et al.*, 1993; Sultan, 1996]. In the context of this study, a higher altitude of the equatorial F layer implies a larger value of l , and hence greater loss of signal in propagation between E and F regions for a given k_z , than when the height of the equatorial F layer is low. Thus, for a given E region conductivity, a large vertical upward drift near sunset which takes the equatorial F region to greater heights should help the growth of equatorial bubbles.

The present model is a simplified picture of how the coupling between the equatorial F region and the con-

jugate E regions affects the development of equatorial bubbles. A three-dimensional model in which variations in the vertical (x) direction are introduced would allow the use of a realistic profile for the vertical gradient in plasma density. The effects of neutral winds must be incorporated as well as possible hemispherical asymmetries in the background propagation medium. This last factor could change significantly the condition of near alignment of the solar terminator with the magnetic meridian. The present study has made use of the basic equations with some simplifying assumptions, for example, that the propagation medium has no variations along the geomagnetic field direction, to obtain wave equations for the propagation of Alfvén waves in the background plasma. Also, reflection of the Alfvén waves from the E regions and the generator region has been considered to be equivalent to closure of the FACs carried by the Alfvén waves into those regions. This treatment nevertheless demonstrates that inclusion of magnetic field fluctuations is important because they are associated with Alfvén waves which carry the FACs into the E regions. This also introduces the characteristics of the medium between the equatorial F region and the conjugate E regions into the problem. A proper treatment of the nonlinear evolution of ESF bubbles should not, therefore, be restricted to an electrostatic instability and should include a more realistic description of the reflection of Alfvén waves from the generator region as well as the conjugate E regions, where longitudinal gradients are present in the Pedersen conductivities.

Acknowledgments. This work was performed while A. Bhattacharyya held a National Research Council-AFRL senior research associateship and was also supported by the Air Force Office of Scientific Research Task 2311PL013.

Janet G. Luhmann thanks Michael J. Keskinen and another referee for their assistance in evaluating this paper.

References

- Abdu, M. A., I. S. Batista, and J. H. A. Sobral, A new aspect of magnetic declination control of equatorial spread F and F region dynamo, *J. Geophys. Res.*, **97**, 14,897-14,904, 1992.
- Aggson, T. L., W. J. Burke, N. C. Maynard, W. B. Hanson, P. C. Anderson, J. A. Slavin, W. R. Hoegy, and J. L. Saba, Equatorial bubbles updrafting at supersonic speeds, *J. Geophys. Res.*, **97**, 8581-8590, 1992.
- Basu, B., and B. Coppi, Relevance of plasma and neutral wind velocities to the topology and the excitation of modes for the onset of the equatorial spread F , *J. Geophys. Res.*, **104**, 225-231, 1999.
- Basu, S., et al., Scintillations, plasma drifts, and neutral winds in the equatorial ionosphere after sunset, *J. Geophys. Res.*, **101**, 26,795-26,809, 1996.
- Fejer, B. G., L. Scherliess, and E. R. de Paula, Effects of the vertical plasma drift velocity on the generation and evolution of equatorial spread F , *J. Geophys. Res.*, **104**, 19,859-19,869, 1999.
- Jackson, J. D., *Classical Electrodynamics*, John Wiley, New York, p. 262, 1975.
- Jayachandran, B., N. Balan, P. B. Rao, J. H. Sastri, and G.

- J. Bailey, HF Doppler and ionosonde observations on the onset conditions of equatorial spread *F*, *J. Geophys. Res.*, *98*, 13,741-13,750, 1993.
- Kan, J. R., and W. Sun, Simulation of the westward traveling surge and Pi 2 pulsations during substorms, *J. Geophys. Res.*, *90*, 10,911-10,922, 1985.
- Kelley, M. C., *The Earth's Ionosphere: Plasma Physics and Electrodynamics, Int. Geophys. Ser., vol. 34*, Academic, San Diego, Calif., 1989.
- Kelley, M. C., and T. Maruyama, A diagnostic model for equatorial spread *F*, 2. The effect of magnetic activity, *J. Geophys. Res.*, *97*, 1271-1277, 1992.
- Keskinen, M. J., S. L. Ossakow, S. Basu, and P. J. Sultan, Magnetic-flux-tube-integrated evolution of equatorial ionospheric plasma bubbles, *J. Geophys. Res.*, *103*, 3957-3967, 1998.
- Ossakow, S. L., Spread *F* theories - A review, *J. Atmos. Terr. Phys.*, *43*, 437-452, 1981.
- Sato, T., and T. E. Holzer, Quiet auroral arcs and electrodynamic coupling between the ionosphere and the magnetosphere, *J. Geophys. Res.*, *78*, 7314-7329, 1973.
- Sultan, P. J., Linear theory and modeling of the Rayleigh-Taylor instability leading to the occurrence of equatorial spread *F*, *J. Geophys. Res.*, *101*, 26,875-26,891, 1996.
- Tsunoda, R. T., Control of the seasonal and longitudinal occurrence of equatorial scintillations by the longitudinal gradient in integrated *E* region Pedersen conductivity, *J. Geophys. Res.*, *90*, 447-456, 1985.
- Weber, E. J., et al., Equatorial plasma depletion precursor signatures and onset observed at 11° south of the magnetic equator, *J. Geophys. Res.*, *101*, 26,829-26,838, 1996.
- Zalesak, S. T., S. L. Ossakow, and P. K. Chaturvedi, Non-linear equatorial spread *F*: The effect of neutral winds and background Pedersen conductivity, *J. Geophys. Res.*, *87*, 151-166, 1982.
-
- A. Bhattacharyya and W. J. Burke, Air Force Research Laboratory, 29 Randolph Road, Hanscom AFB, MA, 01731-3010. (archana@iig.iigm.res.in; william.burke2@hanscom.af.mil)

(Received December 23, 1999; revised March 22, 2000; accepted April 25, 2000.)